Tetrahedron 84 (2021) 132017

Contents lists available at ScienceDirect

Tetrahedron

journal homepage: www.elsevier.com/locate/tet

Stereospecific *N*-acylation of indoles and corresponding microwave mediated synthesis of pyrazinoindoles using hexafluoroisopropanol

Aarushi Singh [a], Snigdha Singh [a, b], Shubham Sewariya [a], Nidhi Singh [a], Prashant Singh [c], Ajay Kumar [d], Rakeshwar Bandichhor [e], Ramesh Chandra [a, f, *]

[a] Laboratory of Drug Discovery and Development, Department of Chemistry, University of Delhi, Delhi, 110007, India
[b] Chemistry Research Laboratory, University of Oxford, 12 Mansfield Road, Oxford, OX1 3TA, United Kingdom
[c] Department of Chemistry, Atma Ram Sanatan Dharma (ARSD) College, University of Delhi, New Delhi, 110021, India
[d] Department of Chemistry, Indian Institute of Technology (IIT), Delhi, 110016, India
[e] Dr. Reddy's Laboratories, Limited, Innovation Plaza, IPDO Bachupally, Hyderabad, 500090, India
[f] Dr. B.R. Ambedkar Center for Biomedical Research, University of Delhi, Delhi, 110007, India

ARTICLE INFO

Article history:
Received 30 November 2020
Received in revised form
31 January 2021
Accepted 5 February 2021
Available online 15 February 2021

Keywords:
Hexafluoroisopropanol
Stereospecific
Pictet-spengler reaction
Microwave

ABSTRACT

We envisioned a facile construction of diversified pyrazinoindoles by using 1,1,1,3,3,3-Hexafluoroisopropanol (HFIP) as the solvent and catalyst, hence eliminating metal catalyzed routes for its development. The process is facilitated by HFIP that has emerged as a powerful tool for development of novel fused heterocycles. This cascade approach blends the asymmetric *N*-acylation with consecutive intramolecular cyclisation via Pictet-Spengler reaction as an efficient tool forming overall two stereogenic centers. Our approach deals with incorporation of L-amino acid on substituted indoles to provide the chiral *N*-acylated indole precursor followed by cyclisation to access pyrazinoindole derivatives in high enantiomeric excess up to >99% in good to excellent yields, which have great potential as molecular scaffolds in drug discovery. We have also described the mechanistic course of the reaction based on density functional theory.

1. Introduction

Heterocycles bearing stereocenters are common structural motifs in biologically active compounds [1] and over the year's various innovative synthetic methods for their synthesis have been reported [2,3]. Approaches to synthesize nitrogen-containing functionalities are of great importance [4,5], not only form the view point of significant functional group but also owing to their vast structural assortments to act as a versatile precursor in various organic reactions [6]. Amongst the widely distributed fused indole heterocycles in various alkaloids and natural product synthesis, pyrazinoindoles are attractive targets for synthetic organic chemists due to their biological activity and ubiquitous structural motifs in natural products [7,8]. The enantiomerically reinforced indole-based heterocycles have a crucial role in medicinal chemistry. Pyrazinoindoles are known to possess wide spectrum of biological activities including receptor agonist, CNS depressant, protein kinase C inhibitor, antibacterial [9–12]. The most common laboratory method used for the synthesis of these indole-based heterocyclic scaffolds involves Pictet-Spengler reaction [13]. The Pictet-Spengler cyclisation [14–17] provides an efficient synthetic method for the synthesis of privileged pharmacophores [17] such as tetrahydro-β-carbolines, tetrahydroisoquinolines or other polyheterocycles [18–20].

Conventionally, the pyrazinoindoles was accessed by Nayak et al. [21] from substituted allylamines and indole-2-carboxaldehyde via saponification followed by Curtius rearrangement. Recently, Wani et al. [22] described an elegant approach for the synthesis of pyrazinoindoles via base mediated ring opening of aziridine with 3-methyl indole followed by $BF_3 \cdot OEt_2$, $MgSO_4$ catalyzed cyclisation. However, applicability of these approaches addresses some issue related to multistep procedure, harsh reaction condition, use of catalyst, thereby limiting their applicability in synthetic chemistry. These challenges are often compounded by socio-economic consequences, however advances in synthetic

* Corresponding author. Dr. B.R. Ambedkar Center for Biomedical Research, University of Delhi, Delhi, 110007, India.
E-mail addresses: rameshchandragroup@gmail.com, acbrdu@hotmail.com (R. Chandra).

https://doi.org/10.1016/j.tet.2021.132017
0040-4020/

organic chemistry offer a realistic means to access such bioactive scaffolds. Despite these elegant developments, exploration of new methods that enables direct access to novel fused indoles from readily available cheap feed stocks would remain highly desirable.

Microwave assisted chemistry has provided an alternate method to conventional synthesis and it is rapidly growing field for organic chemist due to short reaction time, higher yields, high purity products [23]. In the past decade, use of catalyst has exhibited large capacity of complex molecules with good tolerance of functional groups. Although, the use of hexafluoroisopropanol in organic synthesis has become a powerful tool for the development of multicyclic scaffolds [24], and therefore we have eliminated the use of harsh reaction conditions with use of this solvent [25]. Moreover, the hydrogen bonding ability of HFIP along with its enhanced acidity has played an integral part in boosting the reactivity. Whilst scrutiny of various solvent for the cyclisation, HFIP plays a vital role in stimulating cyclisation of pyrazinoindoles through microwave mediated synthesis. The use of HFIP as a solvent for the cyclisation came out as a result of strenuous optimization of various acid catalysts rather than a pre-planned investigation [26]. Several examples are known in the literature for the use of HFIP as a solvent but it sometimes plays a dual role where HFIP has deeper significance under the reaction protocol apart from its use as a solvent without using additional acid catalyst [27–29]. In spite of lacking proper explanation regarding the role of HFIP in the reaction mechanism, this work would pave the way for efficient development of indole-based scaffolds.

Considering the shortcomings in the existing procedures to access these for the synthesis of pyrazinoindoles and pioneering achievements of pyrazinoindoles in the field of medicinal chemistry [30–32]. The enantioselective *N*-acylation of indole has been a grueling task owing to the innate high nucleophilicity at C-3 position and feeble acidity of the N–H bond of the indole nucleus. Therefore, the identification of safe, efficacious, and ecologically sound strategies to achieve the *N*-acylation of indole accounts for an imperative challenge. Interestingly, HFIP promoted cyclisation has eliminated the use of lewis acid catalyst, Brønsted acid and led to the streamlined synthesis of pyrazinoindoles in excellent yields. Following a discussion of the existing state of the art, we aim to develop operationally straightforward, one pot, metal-free and an efficient microwave assisted route to access diastereomeric pyrazinoindole derivatives **4** using HFIP as a solvent via Pictet-Spengler reaction.

2. Result and discussion

In 2006, Tiwari group [33] reported the stable one-pot synthesis of pyrazinoindole from indolyl ethylamine by reacting with aldehydes in presence of lewis acids. Another appealing route to Pyrazinoindole was reported by Padwa group [34] via the gold-catalyzed intramolecular reaction of alkynes (Fig. 1). A third approach, disclosed by the Wani group, again features the construction of pyrazinoindole via base mediated ring opening of aziridines Inspired by these findings, we started our synthesis using readily available feedstock to access pyrazinoindoles.

2.1. Optimization of reaction conditions

Our synthetic journey commenced with *N*-acylation of 3-methyl indole by incorporating amino acids. To achieve an efficient route for *N*-acylation of 3-methyl indole, several conditions were screened. During the initial attempt, 3-methyl indole was coupled with *N*-boc protected amino acid using different coupling reagent. To access pyrazinoindoles, we reduced indole/3-methyl indole to indoline/3-methyl indoline **1(a,b)** using sodium cyanoborohydride

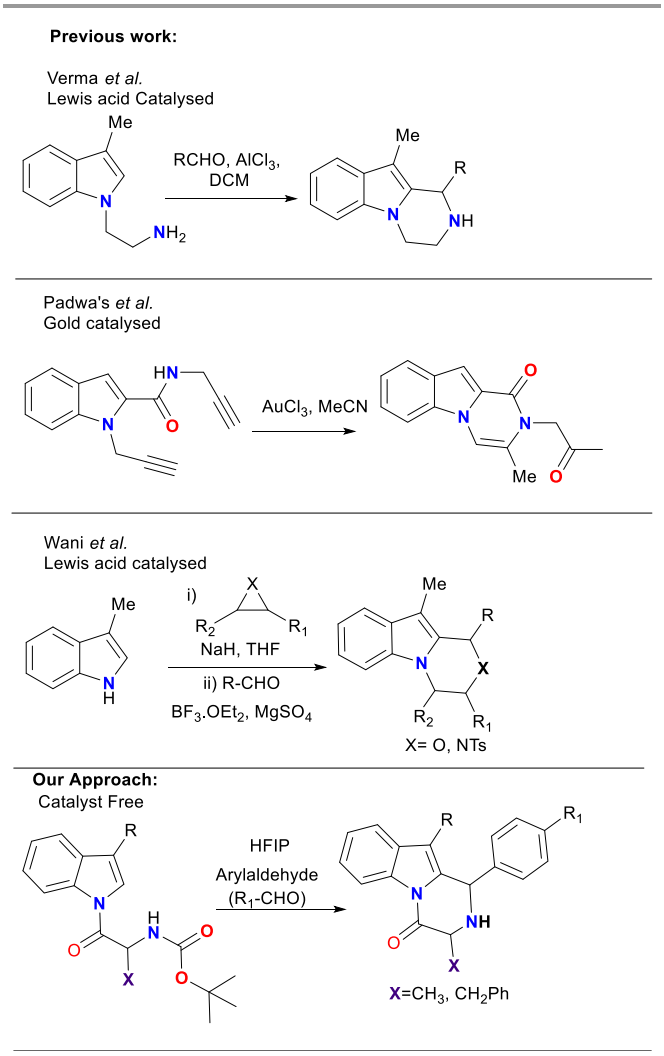

Fig. 1. Previous work and our finding.

in presence of acetic acid [35], which was easily coupled with *N*-boc protected amino acid using common coupling reagents. After obtaining the desired coupled product **2(a–c)**, we aromatized our indoline nucleus using DDQ that afforded our desired precursor **3(a–c)**, which was purified using column chromatography and obtained in good yields [36] (Scheme 1).

We started to optimize our final step with the reaction of *N*-boc protected amine **3a** and 4-nitro benzaldehyde to obtain cyclized product **4a** as depicted in Table 1. We first commenced our reaction by deprotection of the boc protected chiral amines followed by the reaction of chiral amine (1.0 equiv.) and benzaldehyde (1.0 equiv.) in presence of PTSA (1.2 equiv.) as catalyst in DCE at rt for 2 h to obtain **4a** but unfortunately no product formation was observed (Table 1, entry 1). Then, amine (1.0 equiv.) & benzaldehyde (1.0 equiv.) was subjected to 20% acetic acid in MeOH at rt, but we couldn't see product formation even during reflux.

Thereafter we charged our reaction vial with amine, benzaldehyde and dissolved in DCM at rt in presence of $AlCl_3$ and catalytic amount of benzotriazole for 12 h and the corresponding pyrazinoindole derivative **4a** was formed in 18% yield (Table 1, entry 3). To improve the reaction yield, we altered reaction parameters like lewis acid, solvent, temperature and screening of solvents which could led us to HFIP. Due to outstanding feature of HFIP, it could

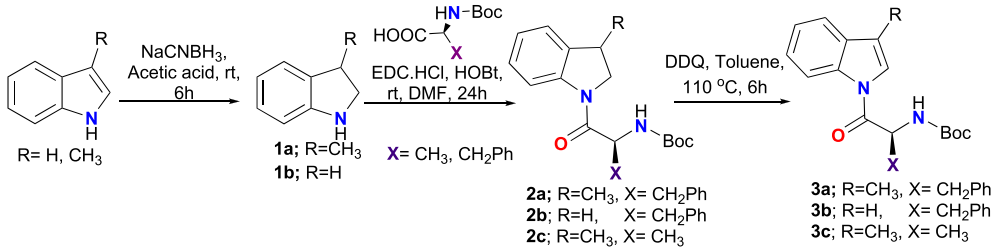

Scheme 1. Synthesis of *N*-acylated chiral amines **3(a–c)** from Indoles and L-amino acids.

Table 1
Optimization of the one-pot reaction to access pyrazinoindole **4a**.

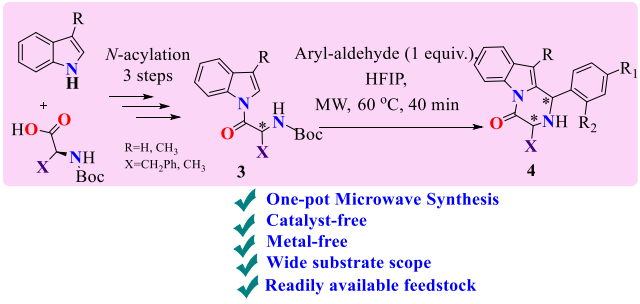

Entry	Reaction Conditions	Product 4a (%)
1.	20%TFA in DCM; PTSA (1.2 equiv.), DCE, rt→reflux, 2–12 h	NR[a]
2.	20%TFA in DCM; MeOH, Acetic acid (20 mol%), rt→reflux, 2–12 h	NR[a]
3.	20%TFA in DCM; cat. amt. $AlCl_3$, Benzotriazole (1.0 equiv.), DCM, rt, 12 h	18%
4.	20%TFA in DCM; cat. amt. $AlCl_3$, Benzotriazole (1.0 equiv.), DCM, 60 °C, 12 h	NR[a]
5.	HFIP, rt, 24 h	NR[a]
6.	HFIP, reflux, 12 h	80
7.	HFIP, 60–65 °C, MW, 40 min	92

[a] NR: no reaction.

easily perform the deprotection of the *N*-Boc group, simultaneously performs cyclisation [37]. Therefore HFIP at refluxing temperature for 12 h yielded 80% product as a single diastereomer (Table 1, entry 6). Encouraged by this result, the similar conditions were employed under microwave irradiation for 40 min which led to improved yield (Table 1, entry 7).

The result of a brief survey of the generality & scope of this one-pot process with chiral amine and aryl aldehyde are summarized in Table 1. The final product was characterized using spectroscopic data and further using X-ray crystal analysis, as depicted in Scheme 2.

2.2. Substrate scope

With the optimized reaction conditions in hand, we investigated the substrate scope of reaction using the aryl aldehyde bearing both electron donating groups (Me, OMe) and electron withdrawing group (nitro, flouro, chloro, bromo) for the synthesis of various substituted pyrazinoindoles in good yields.

Interestingly, we found that electron withdrawing substituents at ortho, para or meta positions of aryl aldehydes (Scheme 2, entries 1–4) and electron-donating (Scheme 2, entry 5) at para position were well tolerated, producing the cyclized products **4**(**a-g**) &**4**(**a'-e'**) in moderate to good yields. Unfortunately, 4-methoxybenzaldehyde (Scheme 2, entry 7) was found to be a poor substrate under these conditions, although elevated temperatures and extended reaction times couldn't acquire the desired product. However, it is important to note that electron withdrawing groups on the aryl aldehyde significantly facilitate the reaction; the final products were obtained in high yields (Scheme 2, entries 1–4, 6). The reaction was found less sensitive to substitution at all ring positions of the aryl aldehyde, with the shortest reaction times observed for para substituted aryl aldehydes (entry 1).

The pyrazinoindole derivatives were also accessed from L-boc alanine amino acid, the desired product were obtained here as a mixture of diastereomers in good yields. The corresponding pyrazinoindoles **4(A–E)** were synthesized by series of aryl aldehydes in good yields with diastereomeric ratio up to 2:1. The *dr* ratios calculated from ^{1}H NMR spectroscopic technique are summarized in Scheme 3.

2.3. Mechanism based on DFT calculations

Authors have tried to propose the mechanism for the formation of the compounds as shown in Scheme 4 based on the DFT approach using Gaussian 9.0. According to our observation, the HFIP initiated the reaction by deprotecting the chiral amine and then free amine attacks on aryl aldehydes generating the corresponding iminium ion, which undergoes cyclisation to give pair of diastereomers by the rotation of the C=N bond. The boat like transition state **P** is bound to attack through C-2 of the indole ring on the prochiral C=N bond in 6-endo-trig approach via two pathways *re*- and *si*-face intramolecular nucleophilic attack.

Herein, intermediate **P** is used to understand the *re* face and *si*

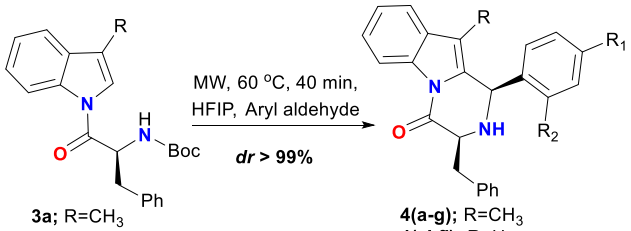

Entry	Code	R	R_1	R_2	Yield(%)	de[b]
1	**4a**	CH_3	NO_2	H	92	99:1
2	**4b**	CH_3	H	NO_2	82	99:1
3	**4c**	CH_3	Cl	H	86	99:1
4	**4d**	CH_3	CF_3	H	79	99:1
5	**4e**	CH_3	CH_3	H	70	99:1
6	**4f**	CH_3	F	F	78	99:1
7	**4g**	CH_3	OCH_3	H	nr	nr
8	**4a'**	H	NO_2	H	87	99:1
9	**4b'**	H	CF_3	H	77	99:1
10	**4c'**	H	Br	H	83	99:1
11	**4d'**	H	F	F	74	99:1
12	**4e'**	H	CH_3	H	46	99:1

[a]Reaction condition: **3(a-b)** (1.038 mmol, 1.0 equiv.), HFIP (1mL) Aryl adehydes (1.038 mmol, 1.0 equiv.): Microwave at 60 °C for 40 min. [b]de: diastereomeric excess; ee: enantiomeric excess calculated from nmr. Products were obtained as single diastereomer confirms de equals to ee.

Scheme 2. Scope for the Synthesis of pyrazinoindoles **4**[a] using L-Phenylalanine based chiral amines **3(a,b)**.

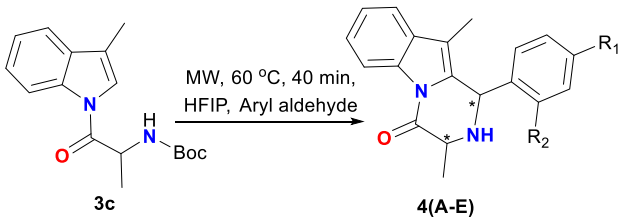

Entry	Code	R_1	R_2	Yield(%)	dr[b]
1	**4A**	CF_3	H	80	1.5:1
2	**4B**	NO_2	H	79	1:1
3	**4C**	Cl	H	82	1:1
4	**4D**	CH_3	H	66	2:1
5	**4E**	F	F	73	2:1

[a]Reaction condition: **3c** (1.038 mmol, 1.0 equiv.), HFIP (1mL) Aryldehydes (1.038 mmol, 1.0 equiv.): Microwave at 60 °C for 40 min. [b]*dr*: diastereomeric ratio; calculated from nmr

Scheme 3. Scope for the Synthesis of pyrazinoindoles 4[a] using L-Alanine based chiral amines **3c**.

face attack to the major and minor product. In case of *re* face attack, **P** gives **B**, a transition state is hypothesized with a free energy change of 5.3 kcal/mol, while in the case of *si* face attack on **P**, it gives another hypothesized transition, **A** with a free energy change of 9.9 kcal/mol (Fig. 2). The transition state, **B** found out to favourable than **A** as lesser the free energy change indicate feasibility of the reaction.

Further, **B** gives a transition state with a free energy change of 0.0 kcal/mol indicating its endothermic character of the reaction while **A** gives an intermediate with a free energy change of −3.4 kcal/mol showing exothermic character. Further, **B** and **A** gives **4** and **4″** with free energy change of 349 and 346 kcal/mol respectively. Based on DFT calculations, the fast formation of transition state **B** (*re*-face attack) is considered favourable where bulky 1,3- substituents are there in pseudoequatorial orientation that avoids the destabilization caused due to 1,3 diaxial interactions, leading to the major 1,3 cis diastereomer **4**. On the other hand the *si*-face attack produces less favourable species **A**, due to destabilization caused by 1,3 diaxial interaction between bulky groups which explains the formation of minor 1,3 trans diastereomer **4"**. However both the diastereomers are formed in case of X = CH_3 due to less steric hindrance in comparison to bulky X = CH_2Ph group which results in the single diastereomeric product.

Even, the intermediate obtained from **B** has high HOMO-LUMO gap than for **A**, therefore, considered more stable and more reactive. Based on this data, it is proposed that **4** is more favourable than the **4"**

3. Experimental section

3.1. Materials

Solvents and reagents were purchased from commercial sources and used without purification for the experiments. Reactions using microwave were run in a closed vial applying a dedicated CEM-Discover monomode microwave apparatus operating at a frequency of 2.45 GHz with continuous irradiation power from 0 to 300 W (CEM Corporation, P.O. Box 200, Matthews, NC 28106). The product purity was assayed using thin-layer chromatography (TLC) on silica get pre-coated plates from Merck. Visualization was done under UV lamp. Product samples in ethyl acetate were loaded on TLC plates and developed in Ethyl acetate/Petroleum ether (1:9, v/v). When slight impurities were detected by iodine vapour/UV light visualization and ninhydrin stain compounds were further purified thrice using column chromatography on neutral alumina gel (CDH). Melting points were determined on Melting point machine M − 560 (Buchi). Single crystals of shelx were used as supplied. A suitable crystal was selected and mounted on a diffractometer. The crystal was kept at a steady T = 293(2) K during data collection. The structure was solved and by using Olex2 [38] as the graphical interface. The model was refined with olex2.refine 1.3-dev [39] using full matrix least squares minimisation on F2. ^1H and ^{13}C nuclear magnetic resonance (NMR) spectra were recorded in $CDCl_3$, DMSO medium on a JEOL ECX-400P NMR at 400 MHz and 100 MHz, respectively at USIC, University of Delhi, using TMS as an internal standard. Chemical shifts are expressed in ppm (δ-scale) and coupling constants (*J*) in Hz. Splitting patterns are described as singlet (s), doublet(d), doublet of doublet (dd), triplet (t), quartet (q) and multiplet (m). The high-resolution mass spectral data was obtained using a Agilent Technology-6530, Accurate mass, Q-TOF LCMS spectrometer at USIC, University of Delhi. Optical rotations were measured on Rudolph Research analytical Autopol II using a 6.0 mL cell with a 100.0 mm path length at 25 °C and are reported as $[\alpha]D^{25}$ (concentration (c) in gm per 100 mL solvent).

3.2. General experimental procedures

3.2.1. General experimental procedure for the synthesis of compound 1

The 3-methyl indole/indole (1.0 equiv.) is dissolved in acetic acid, then sodium cyanoborohydride (5.0 equiv.) was added portion wise at 0 °C and stirred for 3 h at rt under nitrogen atmosphere. The

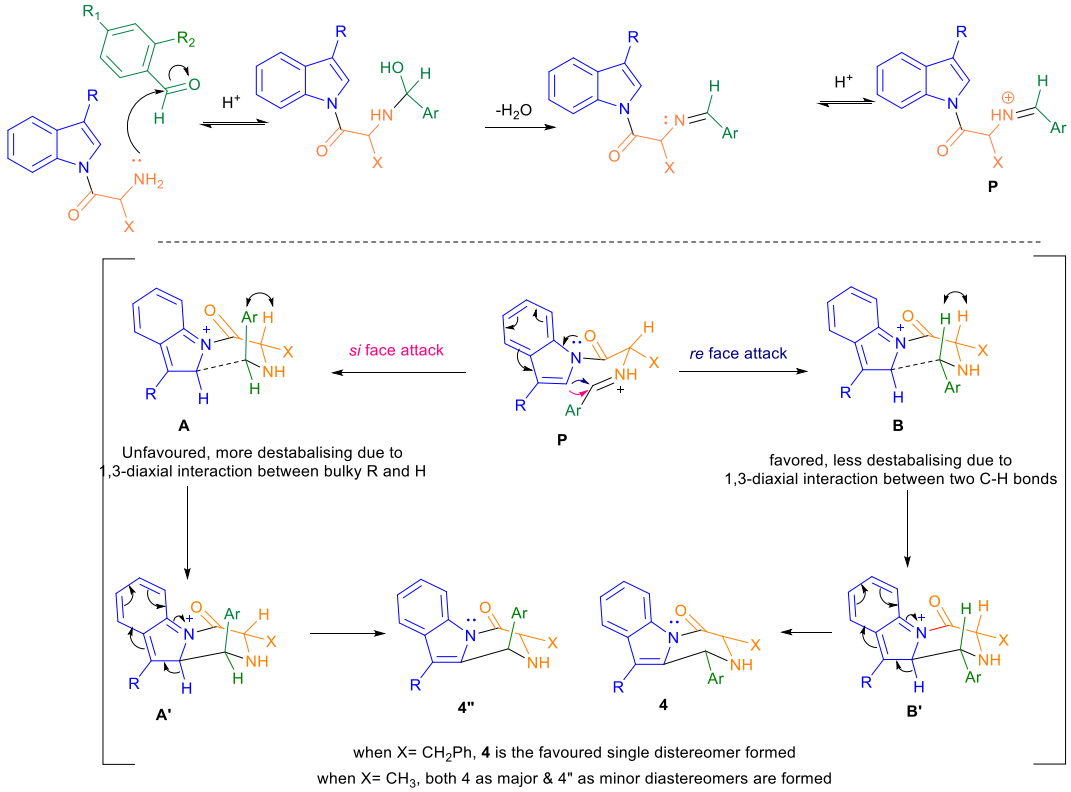

Scheme 4. Plausible Mechanism for Formation of pyrazinoindoles.

completion of reaction was monitored using TLC and the reaction mixture was washed with saturated aq. $NaHCO_3$to neutral pH. The resulting solution was extensively extracted by DCM and the organic solution was washed with brine, dried (Na_2SO_4) and concentrated in vacuo to afford **1** as thick oil.

3.2.2. General experimental procedure for the synthesis of compound 2(a-c)

EDC.HCl (1.2 equiv.), N, N- diisopropylethylamine (2.5 equiv.) were added to a solution of compound **1** (1.0 equiv.), L-boc-amino acid (1.0 equiv.) and HOBt (1.2 equiv.) in dryDMF and stirred for 24 h at rt under nitrogen. To the reaction mixture added EtOAc and the organic solution was washed with water and brine, dried (Na_2SO_4) and concentrated in vacuo. Purification by column chromatography (silica gel, Hexane/EtOAc 95:5) afforded pure **2** as a white solid.

3.2.3. General experimental procedure to access the N-acylated precursors 3(a-c)

To the solution of coupling product **2** (1.0 equiv.) in dried THF, added DDQ (5.0 equiv.) and refluxed for 3–4 h. The completion of reaction was monitored through TLC and the reaction mixture was filtrated through Celite and concentrated over vacuo, purified by column chromatography (silica gel, Hexane/EtOAc 95:5) afforded pure **3** as a white solid.

3.2.4. General experimental procedure to access pyrazinoindoles 4(a-g); 4(a'-f'); 4(A-E)

The designed pyrazinoindoles **4** will be synthesized by using modified Pictet-Spengler reaction. For this, the compound **3(a–c)** (1.038 mmol, 1.0 equiv.) was taken in a clean and dried microwave vial and was charged with minimum amount of HFIP (1 mL) followed by addition of aryl aldehydes (1.038 mmol, 1.0 equiv.). The reaction mixture was set at 60 °C for 40 min to obtain final pyrazinoindoles. The completion of reaction was confirmed using TLC and work up was done by evaporating HFIP twice by adding DCM on reduced pressure. Further it was washed with saturated solution of bisulphite to remove excess of aldehyde. Thus crude obtained was purified using column chromatography on neutral alumina twice due to the presence of aliphatic impurities, we used AR grade solvents throughout out our synthesis and compounds were isolated at 4–6% EtOAc/Hexane to obtain final compounds **4** in fair to good yield.

3.3. Spectroscopic data

3.3.1. tert-butyl(1-(3-methyl-1H-indol-1-yl)-1-oxo-3-phenylpropan-2-yl)carbamate 3a

Melting Point: 128–131 °C. ^{1}H NMR (400 MHz, $CDCl_3$) δ 8.40 (d, J = 7.9 Hz, 1H), 7.48 (d, J = 7.1 Hz, 1H), 7.33 (m, J = 13.7, 7.4, 3.7 Hz, 2H), 7.22–7.16 (m, 4H), 7.12–7.08 (m, 2H), 5.40 (d, J = 8.8 Hz, 1H), 3.15 (m, J = 64.2, 13.8, 6.4 Hz, 2H), 2.21 (s, 3H), 1.40 (s, 9H). ^{13}C NMR (100 MHz, $CDCl_3$) δ 169.98, 155.15, 135.65, 129.48, 128.59, 127.15, 125.46, 124.01, 121.20, 119.48, 118.99, 116.83, 80.27, 54.19, 39.68, 28.36, 9.77. HRMS (ESI-TOF) *m/z*: $[M+Na]^+$ Calcd for $C_{23}H_{26}N_2O_3Na$ 401.1840; found 401.1859. The enantiomeric excess (*ee*) was determined using chiral HPLC analysis (CHIRALPAK IA column, detection at 254 nm), n -hexane/ipropanol = 95:5, flow rate = 1 mL/min, tR (1) = 7.64 min (minor), tR (2) = 8.89 min (major).

3.3.2. tert-butyl(1-(1H-indol-1-yl)-1-oxo-3-phenylpropan-2-yl) carbamate 3b

Melting Point: 99–102 °C. ^{1}H NMR (400 MHz, $CDCl_3$) δ 8.40 (d, J = 8.2 Hz, 1H), 7.53 (d, J = 7.6 Hz, 1H), 7.33 (m., J = 34.2, 21.3, 5.4 Hz, 3H), 7.23 (s, 2H), 7.19 (d, J = 6.6 Hz, 2H), 7.08 (d, J = 7.5 Hz, 2H), 6.58 (d, J = 3.8 Hz, 1H), 5.41–5.23 (m, 2H), 3.23 (m, J = 13.7, 6.3 Hz, 1H),

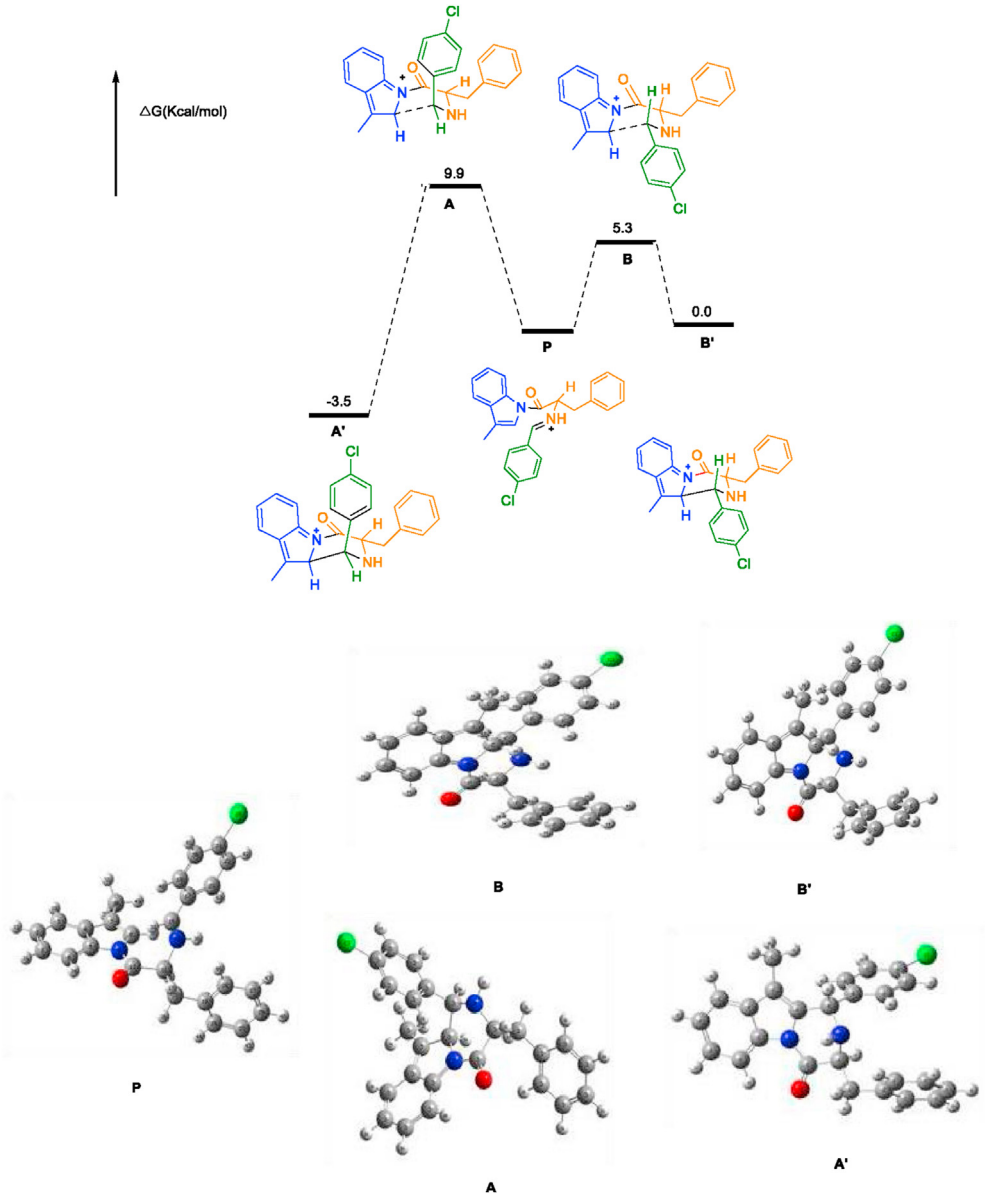

Fig. 2. DFT approach to understand the feasibility of *re-/si*-attack and structures of the intermediates and transition states. Color scheme: N: blue; Cl: green; O: red.

3.06 (m, J = 13.8, 6.2 Hz, 1H), 1.39 (s, 9H). ^{13}C NMR (100 MHz, $CDCl_3$) δ 170.50, 155.15, 135.75, 135.57, 130.62, 129.46, 128.66, 127.22, 125.42, 124.27, 121.02, 116.81, 110.17, 80.35, 54.29, 39.65, 28.37. HRMS (ESI-TOF) *m/z*: $[M+H]^+$ Calcd for $C_{22}H_{24}N_2O_3$ 365.1865; found 365.1851.

3.3.3. *tert-butyl(1-(3-methyl-1H-indol-1-yl)-1-oxopropan-2-yl) carbamate 3c*

Melting Point: 101–103 °C. ^{1}H NMR (400 MHz, $CDCl_3$) δ 8.42 (d, J = 7.9 Hz, 1H), 7.52–7.47 (m, 1H), 7.39–7.33 (m, 1H), 7.31 (dd, J = 7.5, 1.1 Hz, 1H), 7.29–7.26 (m, 1H), 5.47 (d, J = 8.1 Hz, 1H), 5.07 (p, J = 7.1 Hz, 1H) 2.27 (s, 3H), 1.50 (d, J = 7.0 Hz, 3H), 1.44 (s, 9H). ^{13}C NMR (100 MHz, $CDCl_3$) δ 171.33, 155.18, 136.14, 131.63, 125.53, 123.99, 121.13, 119.66, 119.02, 116.85, 80.22, 48.95, 28.42, 19.80, 9.85. HRMS (ESI-TOF) *m/z*: $[M+H]^+$ Calcd for $C_{17}H_{22}N_2O_3$ 303.1708; found 303.1702.

3.3.4. *3-Benzyl-10-methyl-1-(4-nitrophenyl)-2,3-dihydropyrazino [1,2-a]indol-4(1H)-one 4a*

Melting Point: 138–140 °C. ^{1}H NMR (400 MHz, $CDCl_3$) δ 8.47 (dd, J = 8.0, 2.8 Hz, 1H), 8.12 (d, J = 5.2 Hz, 2H), 7.50 (d, J = 7.4 Hz, 1H), 7.42–7.32 (m, 4H), 7.30–7.25 (m, 3H), 7.24 (d, J = 3.7 Hz, 3H), 5.57 (s, 1H), 3.73 (s, 1H), 3.45–3.23 (m, 2H), 2.05 (d, J = 3.0 Hz, 3H). ^{13}C NMR (100 MHz, $CDCl_3$) δ 168.63, 147.72, 145.91, 136.98, 134.70, 131.32, 130.39, 129.60, 128.82, 128.66, 127.13, 125.50, 124.40, 123.97, 118.68, 116.61, 114.12, 55.65, 52.12, 35.85, 8.61. HRMS (ESI-TOF) *m/z*: $[M+H]^+$ Calcd for $C_{25}H_{21}N_3O_3$ 412.1661; found 412.1648. The enantiomeric excess (*ee*) was determined using chiral HPLC analysis (CHIRALPAK IA column, detection at 254 nm), n-hexane/ipropanol = 95:5, flow rate = 1 mL/min, tR (1) = 10.44 min (minor), tR (2) = 12.43 min (major). $[\alpha]_D^{25} = -98.98$ (c = 0.5, $CHCl_3$).

3.3.5. *3-Benzyl-10-methyl-1-(2-nitrophenyl)-2,3-dihydropyrazino [1,2-a]indol-4(1H)-one 4b*

Melting Point: 168–170 °C. ^{1}H NMR (400 MHz, $CDCl_3$) δ 8.45 (d,

J = 8.0 Hz, 1H), 7.81 (dd, J = 7.7, 0.9 Hz, 1H), 7.44 (d, J = 7.5 Hz, 1H), 7.40–7.25 (m, 4H), 7.16 (m, J = 12.9, 5.2 Hz, 3H), 7.08 (d, J = 6.8 Hz, 2H), 6.79 (d, J = 7.4 Hz,1H), 6.07 (s, 1H), 3.48 (s, 1H), 3.16 (m, J = 21.3, 14.0, 5.9 Hz, 2H), 1.96 (s, 3H). ^{13}C NMR (100 MHz, $CDCl_3$) δ 168.78, 149.41, 136.78, 134.66, 133.75, 132.57, 131.18, 130.48, 129.88, 129.52, 129.28, 128.80, 127.01, 125.59, 125.39, 124.33, 118.68, 116.62, 114.18, 55.66, 49.35, 35.82, 8.37. HRMS (ESI-TOF) *m/z*: $[M+H]^+$ Calcd for $C_{25}H_{21}N_3O_3$ 412.1661; found 412.1612. $[\alpha]_D^{25} = -279.09$ (c = 0.5, $CHCl_3$).

3.3.6. 3-Benzyl-1-(4-chlorophenyl)-10-methyl-2,3-dihydropyrazino[1,2-a]indol-4(1H)-one 4c

Melting Point:150–152 °C.^{1}H NMR (400 MHz, $CDCl_3$) δ 8.49–8.45 (m, 1H), 7.51–7.46 (m, 1H), 7.39 (dd, J = 7.4, 1.3 Hz, 1H), 7.36 (dd, J = 3.7, 1.6 Hz, 1H), 7.34–7.30 (m, 1H), 7.28 (s, 1H), 7.26 (d, J = 2.3 Hz, 2H), 7.23 (d, J = 3.6 Hz, 3H), 7.10 (d, J = 8.4 Hz, 2H), 5.49 (s, 1H), 3.79 (d, J = 4.8 Hz, 1H), 3.34 (m, J = 21.1, 13.9, 5.9 Hz, 2H), 2.02 (s, 3H). ^{13}C NMR (100 MHz, $CDCl_3$) δ 169.11, 137.23, 130.43, 129.56, 129.48, 129.12, 129.01, 128.92, 128.77, 126.99, 125.16, 124.20, 118.52, 116.56, 55.42, 52.02, 35.95, 8.51. HRMS (ESI-TOF) *m/z*: $[M+H]^+$ Calcd for $C_{25}H_{21}ClN_2O$ 401.1422; found 401.1441. $[\alpha]_D^{25} = -41.74$ (c = 0.15, $CHCl_3$).

3.3.7. 3-Benzyl-10-methyl-1-(4-(trifluoromethyl)phenyl)-2,3 dihydropyrazino[1,2-a]indol-4(1H)-one 4d

Melting Point:140–142 °C.^{1}H NMR (400 MHz, $CDCl_3$) δ 8.48 (d, J = 8.6 Hz, 1H), 7.53 (dd, J = 8.6 Hz, 3H), 7.40 (dd, J = 7.3, 1.3 Hz,1H), 7.37 (dd, J = 3.9, 1.5 Hz,1H), 7.35–7.32 (m,1H), 7.29 (s,1H), 7.27 (s,3H), 7.23 (s,1H), 7.22 (s,1H), 5.45 (s, 1H), 3.69 (dd, J = 7.7, 4.4 Hz, 1H), 3.35–3.20 (m, 2H), 2.06 (s, 3H). ^{13}C NMR (100 MHz, $CDCl_3$) δ 171.30, 137.09, 134.67, 131.97, 130.51, 129.58, 128.77, 128.00 (q, J_{C-F} = 261 Hz), 127.03, 125.72, 125.27, 124.25, 118.55, 116.56, 113.73, 60.50, 21.15, 14.27, 8.52. ^{19}F NMR (377 MHz, $CDCl_3$) δ −62.58. HRMS (ESI-TOF) *m/z*: $[M+H]^+$ Calcd for $C_{26}H_{21}F_3N_2O$ 435.1684; found 435.1678. $[\alpha]_D^{25} = -96.25$ (c = 0.5, $CHCl_3$).

3.3.8. 3-Benzyl-10-methyl-1-(p-tolyl)-2,3-dihydropyrazino[1,2-a] indol-4(1H)-one 4e

Melting Point: 130–132 °C. ^{1}H NMR (400 MHz, $CDCl_3$) δ 8.48 (d, J = 7.6 Hz, 1H), 7.48 (d, J = 6.9 Hz, 1H), 7.40–7.31 (m, 2H), 7.30–7.25 (m, 2H), 7.22 (d, J = 7.3 Hz, 3H), 7.07 (d, J = 7.8 Hz, 2H), 6.98 (d, J = 7.7 Hz, 2H), 5.40 (s, 1H), 3.78 (dd, J = 7.3, 3.6 Hz, 1H), 3.38 (dd, J = 14.0, 3.6 Hz, 1H), 3.18 (dd, J = 13.8, 8.3 Hz, 1H), 2.31 (s, 3H), 2.03 (s, 3H). ^{13}C NMR (100 MHz, $CDCl_3$) δ 169.35, 137.74, 137.40, 135.66, 134.67, 133.08, 130.86, 129.57, 129.48, 128.76, 127.49, 126.94, 124.94, 124.11, 118.47, 116.54, 113.25, 55.41, 52.41, 36.07, 21.20, 8.51. HRMS (ESI-TOF) *m/z*: $[M+H]^+$ Calcd for $C_{26}H_{24}N_2O$ $C_{26}H_{24}N_2O$ 381.1969; found 381.1961. $[\alpha]_D^{25} = -102.96$ (c = 0.5, $CHCl_3$).

3.3.9. 3-Benzyl-1-(2,4-difluorophenyl)-10-methyl-2,3-dihydropyrazino[1,2-a]indol-4(1H)-one 4f

Melting Point:134–136 °C. ^{1}H NMR (400 MHz, $CDCl_3$) δ 8.43 (d, J = 7.9 Hz, 1H), 7.35–7.26 (m, 3H), 7.21 (dd, J = 16.9, 9.4 Hz, 6H), 6.84–6.73 (m, 2H), 5.34 (s, 1H), 3.95 (dd, J = 8.7, 2.8 Hz, 1H), 3.60 (dd, J = 14.2, 3.0 Hz, 1H), 2.99 (dd, J = 13.9, 9.2 Hz, 1H), 1.47 (s, 3H). ^{13}C NMR (100 MHz, $CDCl_3$) δ NMR (101 MHz) δ 168.44, 164.11(d, J_{C-F} = 247.1 Hz), 161.62 (d, J_{C-F} = 247.1 Hz), 137.46, 134.20, 132.68, 131.30, 129.51, 128.94, 128.89, 127.05, 125.12, 124.06, 118.28, 116.44, 113.03, 112.43, 112.39, 104.01, 61.18, 50.67, 36.79, 8.21. ^{19}F NMR (377 MHz, $CDCl_3$) δ −111.70, −115.35. HRMS (ESI-TOF) *m/z*: $[M+H]^+$ Calcd for $C_{25}H_{20}F_2N_2O$ 403.1624, found 403.1636. $[\alpha]_D^{25} = -56.99$ (c = 0.25, $CHCl_3$).

3.3.10. 3-Benzyl-1-(4-nitrophenyl)-2,3-dihydropyrazino[1,2-a] indol-4(1H)-one 4a'

Melting Point: 144–146 °C. ^{1}H NMR (400 MHz, $CDCl_3$) δ 8.28 (d, J = 8.6 Hz, 1H), 7.66 (d, J = 1.8 Hz, 1H), 7.43 (d, J = 10.1 Hz, 2H), 7.23 (d, J = 12.0 Hz, 2H), 7.19 (s, 4H), 7.09 (s, 3H), 6.51 (d, J = 3.8 Hz, 1H), 5.30 (d, J = 20.0 Hz, 2H), 3.15 (dd, J = 42.1, 6.4 Hz, 3H). ^{13}C NMR (100 MHz, $CDCl_3$) δ 170.20, 155.34, 142.39, 136.38, 131.85, 129.66, 129.64, 129.62, 129.60, 129.58, 129.54, 129.52, 129.49, 129.47, 129.45, 129.44, 128.60, 127.51, 127.05, 124.67, 124.33, 117.52, 54.32, 47.87, 40.03. HRMS (ESI-TOF) *m/z*: $[M+H]^+$ Calcd for $C_{24}H_{19}N_3O_3$ 398.1426; found 398.1499. $[\alpha]_D^{25} = -48.13$ (c = 0.5, $CHCl_3$).

3.3.11. 3-Benzyl-1-(4-(trifluoromethyl)phenyl)-2,3-dihydropyrazino[1,2-a]indol-4(1H)-one 4b'

Melting Point:132–134 °C. ^{1}H NMR (400 MHz, $CDCl_3$) δ 8.50 (d, J = 8.0 Hz, 1H), 7.58 (d, J = 8.2 Hz, 2H), 7.50 (d, J = 7.6 Hz, 1H), 7.43 (d, J = 8.2 Hz, 2H), 7.38–7.34 (m, 1H), 7.33–7.30 (m, 3H), 7.29–7.25 (m, 3H), 6.20 (s, 1H), 5.45 (s, 1H), 3.93 (dd, J = 9.1, 4.3 Hz, 1H), 3.32 (m, J = 23.1, 14.0, 6.7 Hz, 1H). ^{13}C NMR (100 MHz, $CDCl_3$) δ 169.03, 143.25, 137.58, 137.02, 134.96, 129.41, 129.22, 129.01), 128.39, 127.23, 125.73 (q, J_{c-F} = 262.7 Hz) 125.14, 124.56, 120.59, 116.58, 106.24, 57.81, 52.97, 35.93. ^{19}F NMR (377 MHz, $CDCl_3$) δ −64.04. HRMS (ESI-TOF) *m/z*: $[M+H]^+$ Calcd for $C_{25}H_{19}F_3N_2O$ 421.1529; found 421.1515. $[\alpha]_D^{25} = -31.40$ (c = 0.5, $CHCl_3$).

3.3.12. 3-Benzyl-1-(4-bromophenyl)-2,3-dihydropyrazino[1,2-a] indol-4(1H)-one 4c'

Melting Point: 140–142 °C. ^{1}H NMR (400 MHz, $CDCl_3$) δ 8.48 (d, J = 8.1 Hz, 1H), 7.46 (dd, J = 15.5, 8.0 Hz, 3H), 7.38–7.32 (m, 2H), 7.30 (dd, J = 8.5, 1.9 Hz, 3H), 7.28–7.22 (m, 4H), 7.17 (d, J = 8.2 Hz, 2H), 6.17 (s, 1H), 5.33 (s, 1H), 3.95 (dd, J = 8.8, 4.3 Hz, 1H), 3.36 (dd, J = 14.0, 4.3 Hz, 1H), 3.27 (dd, J = 14.0, 9.0 Hz, 1H). ^{13}C NMR (100 MHz, $CDCl_3$) δ167.59, 136.38, 135.80, 133.81, 130.82, 128.63, 128.28, 128.11, 127.86, 126.12, 123.97, 123.42, 121.38, 119.45, 115.43, 105.14, 56.70, 51.65, 34.71. HRMS (ESI-TOF) *m/z*: $[M+H]^+$ Calcd for $C_{24}H_{19}BrN_2O$ 431.0761; found 431.0751. $[\alpha]_D^{25} = +27.39$ (c = 0.5, $CHCl_3$).

3.3.13. 3-Benzyl-1-(2,4-difluorophenyl)-2,3-dihydropyrazino[1,2-a] indol-4(1H)-one 4d'

Melting Point:136–138 °C. ^{1}H NMR (400 MHz, $CDCl_3$) δ 8.48 (d, J = 8.1 Hz, 1H), 7.50 (dd, J = 14.9, 8.0 Hz, 1H), 7.39 (t, J = 7.5 Hz, 1H), 7.33 (dd, J = 10.6, 6.1 Hz, 5H), 7.26 (d, J = 8.0 Hz, 2H), 6.95–6.81 (m, 2H), 5.84 (s, 1H), 5.37 (s, 1H), 4.14–4.04 (m, 1H), 3.74 (dd, J = 14.0, 2.9 Hz, 1H), 3.11 (dd, J = 13.9, 9.2 Hz, 1H). ^{13}C NMR (100 MHz, $CDCl_3$) δ 168.46, 130.69, 130.64, 130.60, 130.54, 129.54, 129.29, 129.04, 127.16, 124.93, 124.39, 120.47, 116.36, 105.28, 61.97, 51.15, 36.91. ^{19}F NMR (377 MHz, $CDCl_3$) δ −108.72, −113.86. HRMS (ESI-TOF) *m/z*: $[M+H]^+$ Calcd for $C_{24}H_{18}F_2N_2O$ 389.1465; found 389.1459. $[\alpha]_D^{25} = +20.34$ (c = 0.25, $CHCl_3$).

3.3.14. 3-Benzyl-1-(p-tolyl)-2,3-dihydropyrazino[1,2-a]indol-4(1H)-one 4e'

Melting Point: 152–154 °C. ^{1}H NMR (400 MHz, $CDCl_3$) δ 8.49 (d, J = 8.1 Hz, 1H), 7.51–7.44 (m, 1H), 7.37–7.32 (m, 2H), 7.32–7.27 (m, 4H), 7.15 (dd, J = 19.2, 8.1 Hz, 4H), 6.16 (s, 1H), 5.37 (s, 1H), 4.00 (dd, J = 9.2, 4.3 Hz, 1H), 3.32- (m, J = 23.4, 14.0, 6.8 Hz, 2H), 2.33 (s, 3H). ^{13}C NMR (100 MHz, $CDCl_3$) δ 169.03, 143.25, 137.58, 137.02, 134.96, 129.41, 129.22, 129.00, 128.39, 127.23, 125.79, 125.75, 125.72, 125.68, 125.14, 124.56, 120.59, 116.58, 106.24, 57.81, 52.97, 35.93, 29.81. HRMS (ESI-TOF) *m/z*: $[M+H]^+$ Calcd for $C_{25}H_{22}N_2O$ 367.1810; found 367.1807. $[\alpha]_D^{25} = -41.70$ (c = 0.5, $CHCl_3$).

3.3.15. 3,10-Dimethyl-1-(4-(trifluoromethyl)phenyl)-2,3-dihydropyrazino[1,2-a]indol-4(1H)-one 4A

Melting Point:100–102 °C. ^{1}H NMR (400 MHz, $CDCl_3$) δ 8.50 (dd, J = 10.0, 7.9 Hz, 1H), 7.39 (dd, J = 11.6, 4.4 Hz, 1H), 7.33 (dt, J = 16.1, 4.5 Hz, 3H), 7.26–7.19 (m, 2H), 7.14 (s, 1H) 5.12 (s, 1H), 3.85 (q, J = 6.7 Hz, 1H), 2.40 (s, 3H), 1.56 (d, J = 6.7 Hz, 3H). ^{13}C NMR (100 MHz, $CDCl_3$) δ 169.79, 169.73, 138.12, 136.51, 134.43, 134.36, 134.22, 133.58, 133.56, 132.68, 131.30, 130.57, 130.46, 130.18, 129.22, 129.21, 128.87, 125.14, 125.08, 124.15, 123.95, 118.49, 118.30, 116.53, 116.38, 113.35, 113.33, 60.50, 58.36, 52.25, 50.31, 16.73, 16.67, 8.86, 8.45. ^{19}F NMR (377 MHz, CDCl3) δ −62.58, −62.59. HRMS (ESI-TOF) *m/z*: $[M+H]^+$ Calcd for $C_{20}H_{17}F_3N_2O$ 359.1373; found 359.1376.

3.3.16. 3,10-Dimethyl-1-(4-nitrophenyl)-2,3-dihydropyrazino[1,2-a]indol-4(1H)-one 4B

Melting Point: 128–130 °C. ^{1}H NMR (400 MHz, $CDCl_3$) δ 8.48–8.40 (m, 1H), 8.23 (d, J = 8.7 Hz, 1H), 8.15 (d, J = 8.8 Hz, 1H), 7.63 (d, J = 8.7 Hz, 1H), 7.54–7.39 (m, 2H), 7.38–7.22 (m, 3H) 5.49 (s, 1H), 3.89 (q, J = 6.7 Hz, 1H), 2.10 (s, 3H), 1.47 (d, J = 6.9 Hz, 3H). ^{13}C NMR (100 MHz, $CDCl_3$) δ 170.46, 169.79, 139.12, 137.51, 134.63, 134.46, 134.20, 133.88, 133.56, 132.68, 131.30, 130.57, 130.46, 130.18, 129.25, 129.22, 128.97, 125.14, 125.08, 124.15, 123.95, 118.49, 118.30, 116.53, 116.38, 113.36, 113.32, 60.52, 58.38, 52.27, 50.33, 16.83, 16.69, 8.96, 8.48. HRMS (ESI-TOF) *m/z*: $[M+H]^+$ Calcd for $C_{19}H_{17}N_3O_3$ 336.1348; found 336.1342.

3.3.17. 1-(4-chlorophenyl)-3,10-dimethyl-2,3-dihydropyrazino[1,2-a]indol-4(1H)-one 4C

Melting Point: 128–130 °C. ^{1}H NMR (400 MHz, $CDCl_3$) δ 8.49–8.40 (m,1H), 7.39 (dd, J = 9.0, 2.8 Hz,3H), 7.37–7.35 (m, 1H), 7.34 (dd, J = 7.3, 1.6 Hz, 1H), 7.29 (dt, J = 8.9, 1.9 Hz, 1H), 7.20 (d, J = 8.5 Hz, 1H), 5.31 (s, 1H), 4.11 (q, J = 7.1 Hz, 1H), 2.05 (s, 3H), 1.54 (d, J = 4.1, 2.6 Hz, 3H). ^{13}C NMR (100 MHz, $CDCl_3$) δ 170.46, 169.79, 139.12, 137.51, 134.63, 134.46, 134.20, 133.88, 133.56, 132.68, 131.30, 130.57, 130.46, 130.18, 129.25, 129.22, 128.97, 125.14, 125.08, 124.15, 123.95, 118.49, 118.30, 116.53, 116.38, 113.36, 113.32, 60.52, 58.38, 55.93, 52.27, 50.33, 16.83, 16.69, 8.96, 8.49. HRMS (ESI-TOF) *m/z*: $[M+H]^+$ Calcd for $C_{19}H_{17}ClN_2O$ 325.1107; found 325.1102.

3.3.18. 3,10-Dimethyl-1-(p-tolyl)-2,3-dihydropyrazino[1,2-a]indol-4(1H)-one 4D

Melting Point:106–108 °C. ^{1}H NMR (400 MHz, $CDCl_3$) δ 8.54–8.47 (m, 1H), 7.43–7.37 (m, 1H), 7.37–7.28 (m,3H), 7.24–7.18 (m, 1H), 7.17–7.11 (m, 2H), 5.12 (s, 1H), 3.86 (q, J = 6.7 Hz, 1H), 2.40 (s, 3H), 2.34 (s, 3H), 1.56 (d, J = 6.8 Hz, 3H). ^{13}C NMR (101 MHz, $CDCl_3$) δ 170.58, 170.08, 138.45, 137.81, 137.49, 136.33, 135.96, 135.04, 134.92, 134.62, 134.24, 133.29, 133.14, 131.51, 130.81, 129.72, 129.51, 129.29, 128.63, 127.72, 124.88, 124.05, 123.85, 121.89, 121.79, 121.69, 119.14, 118.88, 118.43, 118.23, 116.50, 116.37, 115.91, 113.23, 113.10, 111.04, 58.78, 55.97, 52.74, 50.29, 21.36, 21.18, 16.79, 16.70, 8.87, 8.46. HRMS (ESI-TOF) *m/z*: $[M+H]^+$ Calcd for $C_{20}H_{20}N_2O$ 305.1654; found 305.1648.

3.3.19. 1-(2,4-difluorophenyl)-3,10-dimethyl-2,3-dihydropyrazino [1,2-a]indol-4(1H)-one 4E

^{1}H NMR (400 MHz, $CDCl_3$) δ 8.49–8.43 (m, 1H), 7.44–7.35 (m,2H), 7.36–7.26 (m, 2H), 6.96–6.86 (m, 2H), 6.76–6.69 (m, 1H) 5.52 (s, 1H), 3.88 (q, J = 6.7 Hz, 1H), 2.03 (s, 3H), 1.56 (d, J = 1.5 Hz, 2H). ^{13}C NMR (101 MHz, $CDCl_3$) δ 169.76, 169.73, 161.87 (dd), 159.83 (dd) 134.58, 134.26, 132.95, 131.50, 131.44, 131.40, 131.34, 131.21, 130.65, 130.47, 130.42, 130.37, 130.32, 125.19, 125.10, 124.19, 124.00, 123.97, 123.94, 123.53, 123.49, 123.41, 123.36, 122.95, 122.90, 122.81, 122.77, 121.90, 121.66, 119.14, 113.33, 112.88, 112.43, 112.38, 112.21, 112.17, 111.21, 111.17, 111.01, 110.96, 105.07, 104.81, 104.56, 104.49, 104.24, 103.98, 55.95, 51.26, 50.54, 48.02, 47.99, 16.79, 16.76, 8.45, 8.30. ^{19}F NMR (377 MHz, CDCl3) δ −109.05, −109.55, −113.90, −114.54. HRMS (ESI-TOF) *m/z*: $[M+H]^+$ Calcd for $C_{19}H_{16}F_2N_2O$ 327.1309; found 327.1301.

4. Conclusion

In conclusion, we have identified a simple route to generate enantiomerically pure pyrazinoindoles from chiral amines, aryl aldehydes and HFIP that plays dual role under the reaction. A one-pot, highly enantioselective Pictet-Spengler reaction was used to direct the synthesis under microwave-assisted approach. A plausible mechanism for role of HFIP as a solvent and catalyst supported by DFT calculations has also been discussed, which explains the preferential formation of the 1,3 cis diastereomer via fast formation transition state B (free energy change of 5.3 kcal/mol) by favoured *re* face attack. Noticeably derivatives incorporated with L-phenylalanine amino acid lead to the formation of products with excellent stereospecificities (*de*, *ee*>99%), however, in case of L-alanine amino acid the products were obtained as diastereomers with dr up to 2:1 in good yields. A defined library was synthetically accessed that consist of both electron donating and electron withdrawing substituents in order to compare between the effect of the nature of substituent on the biological activity and we are under investigation of their *in vitro, in vivo* activity against various antibacterial strains. From the antibacterial activities reported in literature, it is clear that many of these scaffolds could serve as an inspiration for development of novel antibacterial chemical entities.

Declaration of competing interest

The authors declare that they have no known competing financial interests or personal relationships that could have appeared to influence the work reported in this paper.

Acknowledgment

RC and AS are thankful to DST-SERB (EEQ/2016/000489) for providing financial assistance for conducting research. RC would like to acknowledge University of Delhi for providing support and necessary facilities to carry out research work. AS is thankful to OLEX2 crystallographic software for solving XRD data. NS and SS are grateful to CSIR for providing the fellowship. Snigdha Singh is thankful to ICMR (45/66/2018-PHA/BMS/OL) for providing Senior research fellowship.

Appendix A. Supplementary data

Supplementary data to this article can be found online at https://doi.org/10.1016/j.tet.2021.132017.

References

[1] K.C. Majumdar, S.K. Chattopadhyay, Heterocycles in Natural Product Synthesis, Wiley-VCH Verlag, 2011.
[2] Z.P. Wang, Q. Wu, J. Jiang, Z.R. Li, X.J. Peng, P.L. Shao, Y. He, Catalytic asymmetric synthesis of pyrrolidine derivatives bearing heteroatom-substituted quaternary stereocenters, Org. Chem. Front. 5 (2018) 36–40.
[3] D. Zheng, A. Studer, Asymmetric synthesis of heterocyclic γ-amino-acid and diamine derivatives by three-component radical cascade reactions, Angew. Chem. 131 (2019) 15950–15954.
[4] E. Vitaku, D.T. Smith, J.T. Njardarson, Analysis of the structural diversity,substitution patterns, and frequency of nitrogen heterocycles among U.S. FDAapproved pharmaceuticals, J. Med. Chem. 57 (2014) 10257–10274.

[5] M.G. Vinogradov, O.V. Turova, S.G. Zlotin, Recent advances in the asymmetric synthesis of pharmacology-relevant nitrogen heterocycles via stereoselective aza-Michael reactions, Org. Biomol. Chem. 17 (2019) 3670–3708.
[6] L. Wei, C. Shen, Y.Z. Hu, H.Y. Tao, C.J. Wang, Enantioselective synthesis of multi-nitrogen-containing heterocycles using azoalkenes as key intermediates, *Chem. Commun.* 55 (2019) 6672–6684.
[7] R.K. Tiwari, A.K. Verma, A.K. Chhillar, D. Singh, J. Singh, V.K. Sankar, V. Yadav, G.L. Sharma, R. Chandra, Synthesis and antifungal activity of substituted-10-methyl-1,2,3,4-tetrahydropyrazino[1,2-a]indoles, Bioorg. Med. Chem. 14 (2006) 2747–2752.
[8] R.K. Tiwari, D. Singh, J. Singh, V. Yadav, A.K. Pathak, R. Dabur, A.K. Chhillar, R. Singh, G.L. Sharma, R. Chandra, A.K. Verma, Synthesis and antibacterial activity of substituted 1,2,3,4-tetrahydropyrazino [1,2-a] indoles, Bioorg. Med. Chem. 16 (2006) 413–416.
[9] E.A. Sokolova, A.A. Festa, Synthesis of pyrazino[1,2-a]indoles and indolo-[1,2-a]quinoxalines, Chem. Heterocycl. Compd. 52 (2016) 219–221.
[10] J. Chang-Fong, J. Addo, M. Dukat, C. Smith, N.A. Mitchell, K. Herrick-Davis, M. Teitler, R.A. Glennon, Evaluation of isotryptamine derivatives at 5-HT2 serotonin receptors, Bioorg. Med. Chem. Lett 12 (2002) 155–158.
[11] F. Cafieri, E. Fattorusso, O. Taglialatela-Scafati, Novel bromopyrrole alkaloids from the Sponge Agelasdispar, J. Nat. Prod. 61 (1998) 122–125.
[12] A.R. Katritzky, A.K. Verma, H.Y. He, R. Chandra, Novel synthesis of 1,2,3,4-Tetrahydropyrazino[1,2-a]indoles, Chem. Commun. 47 (2011) 3625–3627.
[13] A. Calcaterra, L. Mangiardi, G.D. Monache, D. Quaglio, S. Balducci, S. Berardozzi, A. Iazzetti, R. Franzini, B. Botta, F. Ghirga, The pictet-spengler reaction updates its habits, Molecules 25 (2020) 414–496.
[14] A. Pictet, T. Spengler, Über die Bildung von Iso-chinolinderivatendurch Einwirkung von Methylal auf Phenyl-äthylamin, Phenyl-alanin und Tyrosin, Ber. Dtsch. *Chem. Ges* 44 (1911) 2030–2036.
[15] G.J. Tatsui, Preparation of 1-methyl-1,2,3,4-tetrahydro-β- carboline, J. Pharm. Soc. Jpn. 48 (1928) 92.
[16] E.D. Cox, J.M. Cook, The pictet-spengler condensation: a new direction for an old reaction, Chem. Rev. 95 (1995) 1797–1842.
[17] S.J. Gharpure, A.M. Sathiyanarayanan, Stereoselective synthesisof oxazino[4,3-a]indoles employing the oxa-Pictet–Spengler reactionof indoles bearing N-tethered vinylogous carbonate, Chem. Commun. 47 (2011) 3625–3627.
[18] R.N. Rao, B. Maiti, K. Chanda, Application of Pictet–Spengler reaction to indole-based alkaloids containing tetrahydro-β-carboline scaffold in combinatorial chemistry, ACS Comb. Sci. 19 (2017) 199–228.
[19] X. Li, D. Chen, H. Gu, X. Lin, Enantioselective synthesis of benzazepinoindoles bearing trifluoromethylated quaternary Stereo centers Catalyzed by chiral spirocyclic phosphoric acids, Chem. Commun. 50 (2014) 7538–7541.
[20] R.S. Klausen, E.N. Jacobsen, Weak brønsted Acid–Thiourea Co-catalysis: enantioselective, catalytic protio-Pictet–Spengler reactions, Org. Lett. 11 (2009) 887–890.
[21] M. Nayak, G. Pandey, S. Batra, Synthesis of pyrrolo[1,2-a]pyrazines and pyrazino[1,2-a]indoles by Curtius reaction in Morita-Baylis-Hilman derivatives, Tetrahedron 67 (2011) 7563–7569.
[22] I.A. Wani, S. Das, S. Mondal, M.K. Ghorai, Stereoselective construction of pyrazinoindoles and oxazinoindoles via ring-opening/pictet-spengler reaction of aziridines and epoxides with 3-methylindoles and carbonyls, J. Org. Chem. 83 (2018) 14553–14567.
[23] R. Toche, S. Chavan, R. Janrao, Microwave-assisted synthesis of fused tricyclic pyrazino[1,2-a]indole derivatives, Monatsh. Chem. 145 (2014) 1507–1512.
[24] Z. Li, B. Yu, HFIP-promoted de novo assembly of biologically relevant unnatural α-arylated amino esters and dipeptide mimetics, Chem. Eur J. 25 (2019) 16528–16532.
[25] S.K. Sinha, T. Bhattacharya, D. Maiti, Role of hexafluoroisopropanol in C–H activation, React. Chem. Eng. 4 (2019) 244–253.
[26] T. Kida, S.I. Sato, H. Yoshida, A. Teragaki, M. Akashi, 1,1,1,3,3,3-Hexafluoro-2-propanol (HFIP) as a novel and effective solvent to facilely prepare cyclodextrin-assembled materials, Chem. Commun. 50 (2014) 14245–14258.
[27] I. Colomer, A.E.R. Chamberlain, M.B. Haughey, T.J. Donohoe, Hexafluoroisopropanol as a highly versatile solvent, Nat. Rev. 1 (88) (2017) 1–12.
[28] I. Colomer, C. Batchelor-McAuley, B. Odell, T.J. Donohoe, R.G. Compton, Hydrogen bonding to hexafluoroisopropanol controls the oxidative strength of hypervalent iodine reagents, J. Am. Chem. Soc. 138 (2016) 8855–8861.
[29] L.N. Wang, S.L. Shen, J. Qu, Simple and efficient synthesis of tetrahydro-β-carbolines via the pictet–spengler reaction in1,1,1,3,3,3-hexafluoro-2-propanol (HFIP), RSC Adv. 4 (2014) 30733–30741.
[30] B.G.M. Youssif, M.H. Abdelrahman, A.H. Abdelazeem, M.A. Abdelgawad, H.M. Ibrahim, O.I.A. Salem, M.F.A. Mohamed, L. Treambleau, S.N.A. Bukhari, Design, synthesis, mechanistic and histopathological studies of small-molecules of novel indole-2-carboxamides and pyrazino[1,2-a]indol-1(2H)-ones as potential anticancer agents effecting the reactive oxygen species production, Eur. J. Med. Chem. 146 (2018) 260–273.
[31] A.A. Festa, R.R. Zalte, N.E. Golantsov, A.V. Varlamov, E.V.V. der Eycken, L.G. Voskressensky, Alcohol-initiated dinitrile cyclization in basic media:A route toward pyrazino[1,2-a]indole-3-amines, J. Org. Chem. 83 (2018) 9305–9311.
[32] R. Romagnoli, P.G. Baraldi, M.D. Carrion, O.C. Lopez, C.L. Cara, D. Preti, M.A. Tabrizi, J. Balzarini, E. Hamel, E. Fabbri, R. Gambari, Discovery of 8-methoxypyrazino[1,2-a]indole as a new potent antiproliferative agent against Human Leukemia K562 cells. A structure-activity relationship study, Lett. Drug Des. Discov. 6 (2009) 298–303.
[33] R.K. Tiwari, J. Singh, D. Singh, A.K. Verma, R. Chandra, Highly efficient one-pot synthesis of 1-substituted-1,2,3,4-tetrahydropyrazino[1,2-a]indoles, Tetrahedron 61 (2005) 9513–9518.
[34] S. Laliberté, P.K. Dornan, A. Chen, Palladium-catalyzed double allylic alkylation of indole-2-hydroxamates:easy access to pyrazino[1,2-a]indole derivatives, Tetrahedron Lett. 51 (2010) 363–366.
[35] Y. Kumar, L. Florvall, Convenient synthesis of indolines by reduction of indoles with sodium cyanoborohydride in carboxylic acids, Synth. Commun. 13 (2007) 489–493.
[36] Z. Zhua, Y. Guo, X. Wang, F. Wu, Y. Wu, Synthesis of fluorinated 3-pyrrolines and pyrroles via [3+2] annulation of N-arylFluorinated imines with allenoates catalyzed by phosphine, J. Fluor. Chem. 195 (2017) 102–107.
[37] J. Choy, S. Jaime-Figueroa, L. Jiang, P. Wagner, Novel practical deprotection of N-boc compounds using fluorinated alcohols, Synth. Commun. 38 (2008) 3840–3853.
[38] O.V. Dolomanov, L.J. Bourhis, R.J. Gildea, J.A.K. Howard, H. Puschmann, Olex2: a complete structure solution, refinement and analysis program, J. Appl. Crystallogr. 42 (2009) 339–341.
[39] L.J. Bourhis, O.V. Dolomanov, R.J. Gildea, J.A.K. Howard, H. Puschmann, The anatomy of a comprehensive constrained, restrained, refinement program for the modern computing environment - olex2 disected, Acta Crystallogr. A A71 (2015) 59–71.